Journal of the European Ceramic Society **19** (1999) 2823–2831
© 1999 Elsevier Science Ltd
Printed in Great Britain. All rights reserved
PII: S0955-2219(99)00060-6
0955-2219/99/$ - see front matter

The Use of MgO as a Densification Aid for α-SiC

D. Foster* and D. P. Thompson

Materials Division, MMME Department, University of Newcastle-upon-Tyne NE1 7RU, UK

(Received 20 May 1998; accepted 21 February 1999)

Abstract

The suitability of MgO as a densification aid for α-SiC has been investigated. Samples of SiC containing additions of MgO, both alone and in combination with $A1_2O_3$ *and* Y_2O_3*, have been hot pressed at temperatures between 1500 and 1900°C and pressureless sintered at temperatures up to 2000°C. The MgO reacts with surface* SiO_2 *from the SiC grains to form a liquid phase which promotes densification by particle rearrangement and solution-reprecipitation processes. With combined additions of MgO,* Al_2O_3 *and* Y_2O_3*, a eutectic in the system* $MgO{-}Al_2O_3{-}Y_2O_3$ *allows extensive liquid formation at ~1700°C independent of the* SiO_2 *content of the SiC powder, enabling efficient densification by hot-pressing. Volatilisation due to reactions between the MgO and the SiC or with the furnace environment, however, oppose densification by pressureless sintering, and must be compensated for by the use of Mg-containing powder beds. © 1999 Elsevier Science Ltd. All rights reserved*

Keywords: hot-pressing, sintering, grain boundaries, SiC, MgO.

1 Introduction

The use of magnesia as a densification aid for silicon carbide has not been explored to any great extent, due to the problems of volatilisation resulting from reactions between magnesia and the silicon carbide[1] and the furnace atmosphere. However, MgO is cheap, readily available and has been established as a successful additive for the densification of other ceramics, such as silicon nitride, both by hot-pressing and pressureless sintering, and this formed the basis for the extensive studies by Trigg on the pressureless sintering of $SiC/A1_2O_3$ mixes using MgO.[2] The present study represents a continuation of this topic, and describes further densification studies on SiC using MgO and MgO mixed with other oxide additives, under conditions where the volatilisation of MgO is controlled.

Additions of MgO, alone and with Y_2O_3 and Al_2O_3 in various combinations, have been used to promote the densification of α-SiC. The presence of these additives in SiC powder compacts is believed to provide a liquid phase at sintering temperatures by reaction with SiO_2 from the SiC grain surfaces. This liquid forms at lower temperatures than those obtained with additions of the established oxide additives Y_2O_3 and Al_2O_3, and has a lower viscosity, thereby reducing the temperature required for densification, and offering a more energy-efficient sintering route with minimal reaction between SiC and the additives, thus limiting the problem of volatilisation. When Si_3N_4 is sintered with MgO, the liquid phase does not recrystallise on cooling but forms a grain boundary glass with a relatively low softening temperature,[3] imposing limitations on the high-temperature properties of the material.[4,5] Similar restrictions were expected to apply to SiC materials densified with MgO-based additions.

2 Materials and Procedure

2.1 Powder preparation

MgO powder (BDH AnalaR) was milled in a cylindrical rubber-lined ball mill using mixed α–β SAlON media and iso-propanol for 90–190 h, then dried and sieved using a 106 μm mesh to reduce aggregate size. This produced an average particle size of ~0·8 μm. Similar milling was also carried out on $A1_2O_3$ powder (Alcoa grade A17) and Y_2O_3 powder (HC Starck standard grade). The additives were then mixed with α-SiC (HC Starck grade A10), consisting mainly of the 6H polytype with a small level of 15R, by re-milling for approximately 80 h, drying and sieving. Cylindrical "green" pellets were formed by uniaxially pressing the powder mixtures in a steel die under a pressure of 94 MPa.

---

*To whom correspondence should be addressed.

The pellets were then isostatically pressed at a pressure of 172 MPa in thin-walled rubber containers, resulting in powder compacts typically of density 2·01 g cm^{-3}.

2.2 Densification experiments

Uniaxial hot-pressing was carried out in an inductively heated graphite die, in a self-generated atmosphere of CO/N_2, with a layer of BN acting as a pressure-transmitting medium and minimising attack by the carbon at high temperature. A pressure of 29 MPa was maintained on the sample during the heating and hold periods but was released during cooling. The temperature was measured by an infra-red pyrometer sighted on the die (assuming a graphite emissivity of 0·80), allowing the hold temperature to be maintained within ±10°C. A hold time of 30 min was used except where stated. A heating rate of ~30°C min^{-1} was used and the initial natural furnace cooling rate was ~40°C min^{-1}. The shrinkage of the sample was monitored as densification proceeded using a displacement transducer attached to the hot-press. These data were adjusted to allow for the compaction of the hot-press set-up and the gradual loss of pressure from the hydraulic press. Pressureless sintering was carried out in a graphite resistance furnace, with the sample held in a graphite crucible packed with BN except where stated. After evacuation the furnace was filled with nitrogen at 1 bar and a flow of gas was maintained throughout the run. The temperature was measured using a calibrated thermocouple positioned immediately below the crucible. The heating schedule was controlled automatically and a heating rate of ~45°C min^{-1} was used.

2.3 Sample characterisation

The bulk densities of the specimens were obtained by an immersion method using mercury. The calculation of theoretical densities was made with the assumption that all the starting additives were retained. Phase identification and determination of the approximate proportion of phases and unit-cell dimensions were carried out from X-ray powder photographs obtained using a Hägg–Guiner focusing camera (type XDC-700) and CuK$_{\alpha 1}$ radiation. An LS-20 laser line scanner (KEJ instruments) and Scanpi and PIRUM software were used to analyse the reflections. The intensities of the phases are given on a scale of 0–10, with the strongest phase as 10. Phases too weak to be distinguished by the line scanner are assigned as 'W', having an intensity of <0·1. SEM work and energy dispersive X-ray analysis (Link Analytical Systems Ltd) were carried out using a CamScan S4-80DV scanning electron microscope.

3 Results

3.1 Hot-pressing with MgO

Samples of SiC containing 6 and 9 wt% MgO were hot-pressed at hold temperatures of 1750–1900°C (Table 1). Only limited densification (~78% TD) took place at 1750–1850°C. The MgO identified by XRD analysis in these samples appears as large inclusions resulting from aggregates in the powder compact. The presence of a liquid phase during sintering is suggested by the presence of a glassy phase in the XRD results. A log–log plot of the displacement versus time (Fig. 1) rises linearly for about 10 min, starting at around 1700°C. The slope of 1.43 is consistent with shrinkage by particle rearrangement in the presence of a liquid phase,[6] and is too high to be accounted for by solid state mechanisms. The maximum shrinkage obtainable by particle rearrangement [6] does not account fully for the densities obtained, however, suggesting that some further densification by solution and reprecipitation has taken place.

At 1900°C the density increases significantly to 90%TD, suggesting a greater volume of liquid and a more efficient solution-reprecipitation stage. This is supported by SEM images of the sintered microstructure, which show a reduction in the number of small (<0·5 μm) SiC grains accompanied by an increase in the number of large (~2 μm), rounded grains.

Little of the glassy phase is retained above 1750°C, the weight loss increasing significantly between 1750 and 1850°C (Table 1). The weight loss at 1900°C was equal to the original weight of the additive, although EDX analysis indicates the retention of significant levels of Mg in the sample (the outer layer of the sample being Mg-depleted). Increasing the additive weight to 10 wt% gave a slight rise in density to 91% TD at 1900°C, although the weight loss also rose. The weight loss was reduced by the introduction of MgO to the powder used to pack the sample in the hot-press die (equal weights of BN and MgO were used). A greater retention of MgO was seen and a density of 95% TD was obtained.

3.2 Hot-pressing with MgO and Al_2O_3

Samples of SiC containing mixtures of MgO and $A1_2O_3$ having a total weight of 6 wt% were hot-pressed at 1750 and 1850°C (Table 2). The densities obtained were significantly greater than with MgO alone. The densification kinetics and SEM images again suggest that liquid phase sintering takes place. At 1750°C the maximum density of 88% TD, obtained with an additive containing 88 mol% MgO, again suggests that solution-reprecipitation takes place. Spinel, $MgAl_2O_4$, is seen as the sole

Table 1. Hot-pressing with MgO (for 30 min)

Additive size (wt%)	*Packing powder*	*Temperature (°C)*	*Weight loss (wt%)*	*Density (g cm^{-3})*	*Theoretical density (g cm^3)*	*XRD results*
6	BN	1750	1·7	2·47	3·24	$6H_{10}\ 15R_{0\cdot3}\ 4H_{0\cdot1}\ MgO_{0\cdot5}\ Glass_s$
6	BN	1850	5·5	2·52	3·24	$6H_{10}\ 15R_{0\cdot4}\ 4H_{0\cdot2}\ MgO_{0\cdot4}\ Glass_w$
6	BN	1900	6·0	2·91	3·24	$6H_{10}\ 15R_{0\cdot6}\ 4H_{0\cdot8}\ MgO_{0\cdot1}$
6	BN/MgO	1900	2·4	3·07	3·24	$6H_{10}\ 15R_{0\cdot8}\ 4H_{2\cdot0}\ MgO_{1\cdot0}$
10	BN	1900	7·3	2·96	3·25	$6H_{10}\ 15R_{0\cdot5}\ 4H_{1\cdot0}\ MgO_{0\cdot5}$

crystalline additive phase except for the sample containing 92 mol% MgO, where MgO is seen. For additives with low MgO contents, the spinel forms in large (~5 μm) grains and remains solid throughout heating, limiting the volume of liquid available.

At 1850°C a maximum density of 93% TD is obtained for an additive containing 88 mol% MgO (Fig. 2). The weight losses are lower than those seen with additions of MgO alone, the fraction of the MgO lost also being lower.

3.3 Hot-pressing with MgO and Y_2O_3

Samples of SiC containing mixtures of MgO and Y_2O_3 having total weights of 6 and 9 wt% were hot-pressed at 1750 and 1850°C (Table 3). With 6 wt% of additive the final densities, weight losses and the relationship between additive composition and sample density were comparable to those seen with MgO and $A1_2O_3$. MgO was seen as the only additive phase for an addition containing 92 mol% MgO. For all other additive compositions a phase J (Table 4), resembling the YAM-type 'J-phase' $Y_4Si_2O_7N_2$ (ICDD card 32-1451) is seen, increasing in quantity with increasing Y_2O_3 content. This phase is also seen in samples hot-pressed with mixtures of MgO, Al_2O_3 and Y_2O_3 (Section 3.4). Clearly nitrogen has been picked up from the hot-press atmosphere, along with some Al from the SiAlON milling media to modify the $Y_4Si_2O_7N_2$ stoichiometry. Liquid phase sintering is again identified as the dominant densification mechanism. SEM images of the more dense samples show the elimination of smaller grains and the isolation of the liquid phase at grain junctions, suggesting an efficient solution-reprecipitation process (Fig. 3). Increasing the additive weight to 9 wt% gave a significant rise in density, the SEM images suggesting a more homogeneous distribution of the liquid phase.

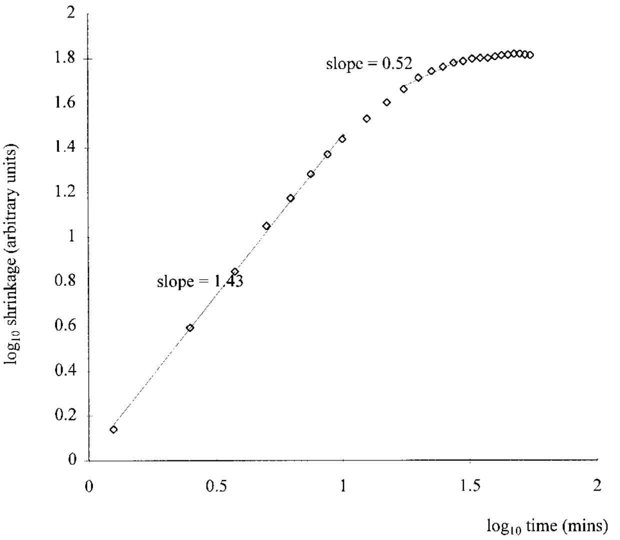

Fig. 1. Log (time) versus log (shrinkage) for SiC hot-pressed at 1900°C with 6 wt% MgO.

3.4 Hot-pressing with MgO, Al_2O_3 and Y_2O_3

Samples of SiC containing mixed additions of MgO, Al_2O_3 and Y_2O_3 with a total additive weight of 9 wt%, were hot-pressed between 1710 and 1850°C (Table 5). Additive compositions with high molar ratios of MgO were investigated, having given optimum densities in additions of MgO plus Al_2O_3 and MgO plus Y_2O_3. Highly dense samples were obtained at 1850°C (up to 99% TD based on the theoretical density of the starting mixture), and good densities were obtained at lower temperatures

Table 2. Hot-pressing with MgO and Al_2O_3 (with 6 wt% of additive for 30 min)

Additive composition (mol%)		*Temperature (°C)*	*Weight loss (wt%)*	*Density (g cm^{-3})*	*Theoretical density (g cm^{-3})*	*XRD results*
MgO	*Al_2O_3*					
92	8	1750	1·7	2·73	3·24	$6H_{10}\ 15R_{0\cdot4}\ 4H_{0\cdot2}\ MgO_{0\cdot3}$
88	12	1750	1·9	2·84	3·24	$6H_{10}\ 15R_{0\cdot4}\ 4H_{0\cdot2}\ MgAl_2O_{4w}$
72	28	1750	1·6	2·68	3·25	$6H_{10}\ 15R_{0\cdot4}\ 4H_{0\cdot1}\ MgAl_2O_{40\cdot2}$
50	50	1750	1·5	2·48	3·25	$6H_{10}\ 15R_{0\cdot3}\ 4H_{0\cdot1}\ MgAl_2O_{40\cdot4}$
88	12	1850	2·6	3·02	3·24	$6H_{10}\ 15R_{0\cdot3}\ 4H_{0\cdot2}\ MgAl_2O_{4w}$
72	28	1850	2·4	3·01	3·24	$6H_{10}\ 15R_{0\cdot5}\ 4H_{0\cdot4}\ MgAl_2O_{40\cdot3}$

(94% TD at 1750°C and 86% TD at 1710°C). The optimum composition was in the range 60–80 mol% MgO, 10–25 mol% Al_2O_3 and 10–25 mol% Y_2O_3. The relatively high densities obtained at 1710°C suggest the presence of an extensive liquid phase. The rate of shrinkage was seen to increase suddenly, indicating liquid formation, typically at a temperature between 1670 and 1720°C although no clear relationship between this temperature and the additive composition was established. Weight losses were reasonably low, rising slightly with the MgO content. Spinel and YAG ($Y_3Al_5O_{12}$) were seen in the XRD results, along with the phase J (Table 4) at Y_2O_3-rich compositions.

The densification mechanisms were further investigated by studying the reaction with respect to temperature (with hold times of 30 min in the range 1500–1900°C) and time (for 5–90 min at 1750°C). An additive weight of 9 wt% and a standard additive composition of 67:16:17 mol% $MgO{:}Al_2O_3{:}Y_2O_3$ were used throughout. The results for the reactions at different temperatures are shown in Table 6. Little densification was seen at 1600°C or below (Fig. 4), although limited particle rearrangement by liquid generated through low-temperature eutectics involving SiO_2 may take place. The density rises rapidly from 82 to 94% TD between 1700 and 1750°C, and gradually continues to approach the full theoretical value at higher temperatures. Weight losses were low except at 1900°C (losing 7 wt%). The phase J was seen as the only crystalline additive phase, increasing in strength with temperature up to 1900°C, where most of the additive is lost through volatilisation. Secondary electron SEM images of the samples (Figs 5 and 6) show a contrast between the core and rim of the SiC grains after hot-pressing at high temperatures. This indicates grain growth by solution and reprecipitation through the liquid phase, the contrast resulting from impurity atoms contained in the material deposited at the rims.[7] The microstructure is homogeneous, with fine (typically $< 2\,\mu m$) rounded grains and the additive phases confined to submicron pockets at grain junctions.

The results for the sequence of samples pressed at 1750°C are shown in Table 7. After only 5 min at 1750°C, limited particle rearrangement and wetting by the liquid phase takes place, resulting in a density of 80% TD. The density rises rapidly with hold time for the first 30 min, but only slowly thereafter (Fig. 7). This is consistent with the kinetic data (Fig. 1). The weight loss reaches 2·2 wt% after

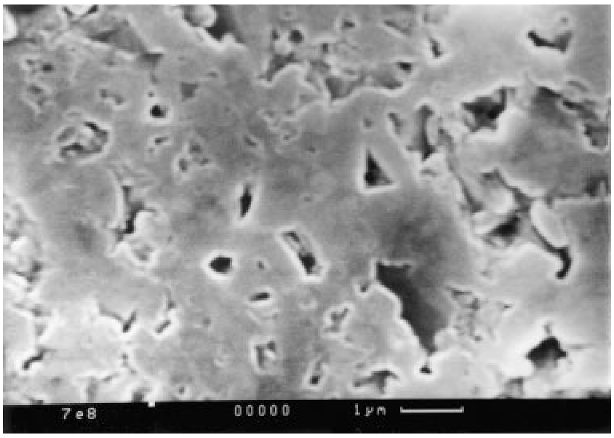

Fig. 2. SiC hot-pressed at 1850°C with 6 wt% of MgO and Al_2O_3 (molar ratio 88:12); sample etched with KOH.

Table 4. *d*-Spacings of XRD patterns for phase J

$Y_4Si_2O_7N_2$ (ICDD card 32-1451)	*Phase J observed with MgO and Y_2O_3*	*Phase J observed with MgO, Al_2O_3 and Y_2O_3*
	$8{\cdot}52_3$	
$7{\cdot}25_{12}$	$7{\cdot}30_2$	$7{\cdot}37_w$
$4{\cdot}53_{15}$	$4{\cdot}60_w$	$4{\cdot}60_w$
	$3{\cdot}50_w$	$3{\cdot}50_w$
$3{\cdot}20_{20}$	$3{\cdot}21_w$	$3{\cdot}26_w$
$3{\cdot}06_{100}$	$3{\cdot}02_{10}$	$3{\cdot}01_{10}$
$2{\cdot}919_{15}$	$2{\cdot}90_w$	$2{\cdot}90_1$
$2{\cdot}864_{30}$		$2{\cdot}87_7$
$2{\cdot}828_{55}$	$2{\cdot}82_9$	
$2{\cdot}519_{16}$		
$2{\cdot}499_{11}$		$2{\cdot}45_w$
$2{\cdot}042_{10}$		$2{\cdot}02_w$
$1{\cdot}979_{15}$		$1{\cdot}96_w$
$1{\cdot}890_{15}$	$1{\cdot}87_2$	$1{\cdot}88_w$
$1{\cdot}815_{14}$		$1{\cdot}81_1$
$1{\cdot}805_{14}$	$1{\cdot}78_w$	$1{\cdot}79_1$

Table 3. Hot-pressing with MgO and Y_2O_3 (for 30 min)[a]

Additive size (wt%)	*Additive composition (mol%)*		*Temperature (°C)*	*Weight loss (wt%)*	*Density (g cm^{-3})*	*Theoretical density (g cm^{-3})*	*XRD results*
	MgO	*Y_2O_3*					
6	92	8	1750	1·8	2·77	3·25	$6H_{10}\,15R_{0{\cdot}6}\,4H_{0{\cdot}1}\,MgO_{0{\cdot}5}$
6	85	15	1750	1·9	2·78	3·26	$6H_{10}\,15R_{0{\cdot}4}\,4H_{0{\cdot}1}\,J_w$
6	68	32	1750	1·3	2·67	3·27	$6H_{10}\,15R_{0{\cdot}5}\,4H_w\,J_{0{\cdot}3}$
6	56	44	1750	0·7	2·63	3·28	$6H_{10}\,15R_{0{\cdot}5}\,4H_w\,J_{0{\cdot}6}$
6	85	15	1850	3·3	3·10	3·26	$6H_{10}\,15R_{0{\cdot}6}\,4H_{0{\cdot}1}\,J_w$
6	68	32	1850	1·9	3·04	3·27	$6H_{10}\,15R_{0{\cdot}5}\,4H_{0{\cdot}2}\,J_{0{\cdot}4}$
9	68	32	1750	0·7	2·98	3·30	$6H_{10}\,15R_{0{\cdot}4}\,4H_{0{\cdot}3}\,J_{0{\cdot}7}$

[a] The phase J resembles the YAM-type 'J-phase' (Table 4).

15 min and does not change significantly thereafter with increasing hold time.

The sample densities were seen to increase with additive weight over the range 3–9 wt% (Table 8). The introduction of MgO, Al_2O_3 and Y_2O_3 (in the same composition as the additive in the sample) to an equal weight of BN in the packing powder gave increased densities, although each sample gained weight suggesting that the oxides in the packing powder form a liquid and infiltrate the sample. SEM images show the microstructure to contain large pockets of the liquid phase and to have undergone little grain growth.

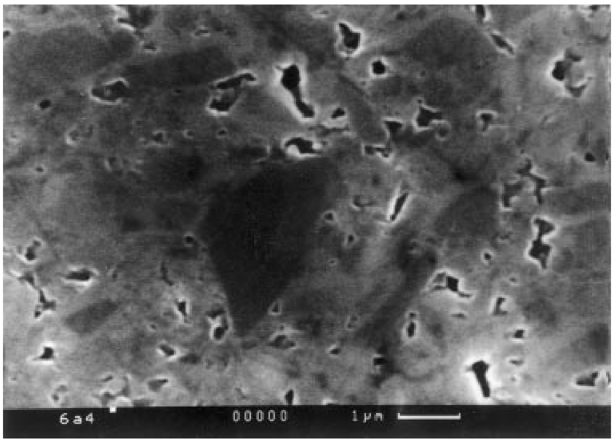

Fig. 3. SiC hot-pressed at 1850°C with 6 wt% of MgO and Y_2O_3 (molar ratio 85:15); sample etched with KOH.

3.5 Pressureless sintering with MgO, Al_2O_3 and Y_2O_3

Samples of SiC containing additions of 9 wt% of MgO, Al_2O_3 and Y_2O_3 in various compositions were pressureless sintered at temperatures between 1750 and 2000°C (Table 9). Two of the samples were sintered in powder beds containing MgO, Al_2O_3 and Y_2O_3 in order to reduce weight loss by volatilisation, whilst the remaining samples were sintered in BN only. Limited densification was achieved at 1750°C, reaching a maximum of 78% TD. The densities obtained at higher temperatures were also low, reaching a value of 86 %TD) after

Table 6. Hot-pressing with 9 wt% of MgO, Al_2O_3 and Y_2O_3 in the molar composition 67:16:17, for 30 min (theoretical density = 3·29 g cm^{-3})

Temp (°C)	*Weight loss (%)*	*Density (g cm^{-3})*	*XRD results*
1500	0·1	2·25	$6H_{10}\,15R_{0\cdot3}\,4H_w$
1600	0	2·33	$6H_{10}\,15R_{0\cdot5}\,4H_w\,J_{0\cdot2}$
1650	0·3	2·48	$6H_{10}\,15R_{0\cdot3}\,4H_{0\cdot2}\,J_{0\cdot2}$
1700	1·0	2·68	$6H_{10}\,15R_{0\cdot3}\,4H_w\,J_{0\cdot4}$
1750	1·6	3·07	$6H_{10}\,15R_{0\cdot6}\,4H_{0\cdot1}\,J_{0\cdot8}$
1800	2·3	3·21	$6H_{10}\,15R_{0\cdot6}\,4H_{0\cdot1}\,J_{1\cdot0}$
1900	7·0	3·23	$6H_{10}\,15R_{0\cdot6}\,4H_{0\cdot4}\,J_{0\cdot5}$

Table 5. Hot-pressing with MgO, Al_2O_3 and Y_2O_3 (with 9 wt% of additive for 30 min) [a]

Additive composition (mol%)			*Temperature (°C)*	*Weight loss (wt%)*	*Density (g cm^{-3})*	*Theoretical density (g cm^{-3})*	*XRD results (additive phases only)*
MgO	*Al_2O_3*	*Y_2O_3*					
42	50	8	1710	0·8	2·58	3·28	—
56	17	27	1710	1·1	2·78	3·30	$J_{0\cdot7}$
64	25	11	1710	1·0	2·82	3·28	$MgAl_2O_{4\,0\cdot1}J_{0\cdot1}$
76	10	13	1710	0·3	2·81	3·28	—
84	11	5	1710	1·3	2·76	3·27	—
37	20	43	1750	1·0	2·86	3·31	$J_{1\cdot0}$
37	43	20	1750	0	2·85	3·29	$YAG_{0\cdot3}$
42	50	8	1750	1·1	2·81	3·28	—
56	8	36	1750	1·0	2·92	3·30	$J_{0\cdot9}$
56	17	27	1750	0·8	2·98	3·30	$J_{0\cdot7}$
56	36	8	1750	1·4	2·94	3·28	$MgAl_2O_{4\,0\cdot3}\,J_w$
64	25	11	1750	2·2	3·09	3·28	$MgAl_2O_{4\,0\cdot1}\,J_{0\cdot2}$
64	25	11	1750	0·6	3·01	3·28	$MgAl_2O_{4\,w}\,J_w$
67	16	17	1750	1·3	3·04	3·29	$J_{0\cdot1}$
67	16	17	1750	1·6	3·07	3·29	$J_{0\cdot7}$
69	8	23	1750	0·7	3·07	3·29	$J_{0\cdot7}$
71	25	4	1750	1·0	2·97	3·27	$MgAl_2O_{4\,0\cdot3}$
76	3	21	1750	1·0	2·97	3·29	$J_{0\cdot9}$
77	10	13	1750	0·9	3·02	3·28	$J_{0\cdot4}$
77	10	13	1750	0·8	2·99	3·28	$J_{0\cdot5}$
77	16	7	1750	1·9	3·05	3·27	$J_{0\cdot2}$
84	5	11	1750	2·0	3·05	3·28	$J_{0\cdot3}$
84	11	5	1750	1·6	2·91	3·27	—
37	43	20	1850	1·8	3·20	3·29	$YAG_{0\cdot5}$
64	25	11	1850	3·0	3·24	3·28	$YAG_{0\cdot4}\,MgAl_2O_{4\,w}$
76	10	13	1850	3·8	3·24	3·28	$J_{0\cdot4}$

[a] The phase J resembles the YAM-type 'J-phase' (Table 4).

sintering at 2000°C comparable to that obtained using an addition of Al_2O_3 and Y_2O_3. The weight losses were high, the powder beds having little beneficial effect. EDX analysis of the samples confirms most of the Mg to be lost during sintering, except at 1750°C.

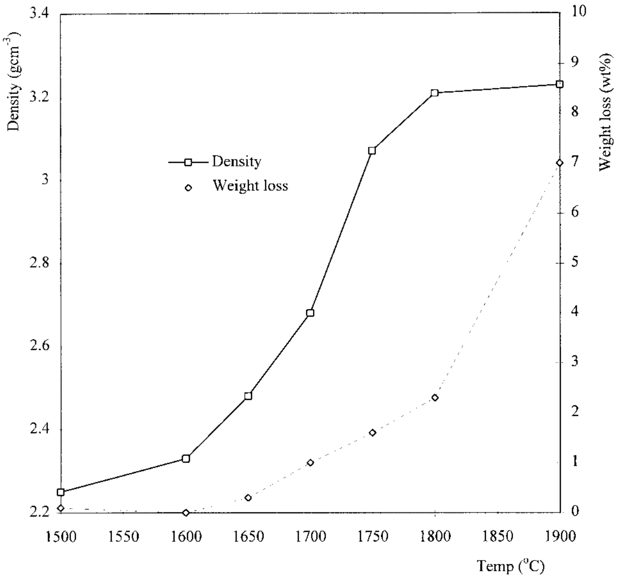

Fig. 4. Hot-pressing for 30 min with 9 wt% of MgO, Al_2O_3 and Y_2O_3 (molar ratio 67:16:17).

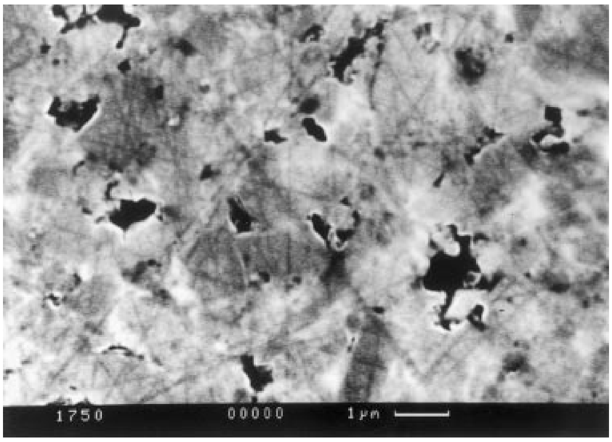

Fig. 5. SiC hot-pressed at 1750°C with 9 wt% of MgO, Al_2O_3 and Y_2O_3 (molar ratio 66:16:17).

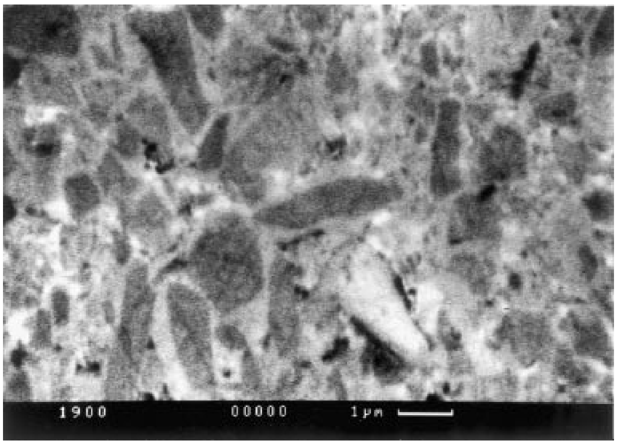

Fig. 6. SiC hot-pressed at 1900°C with 9 wt% of MgO, Al_2O_3 and Y_2O_3 (molar ratio 66:16:17).

4 Discussion

The densification of SiC powder compacts containing oxide additives including MgO can be understood by considering liquid phase sintering processes involving a liquid formed from the additives and surface SiO_2 from the SiC grains.

In the hot-pressing of SiC with MgO only a little liquid is formed below 1700°C, from small MgO grains via the eutectic of composition ~45:55 molar ratio MgO:SiO_2 at 1543°C (Fig. 8). Further liquid is formed at 1695°C, the temperature of the monotectic close to SiO_2, causing the observed increase in the shrinkage rate measured by the displacement transducer attached to the hot-press. A mixture of two immiscible liquids is formed at this temperature, however, causing inhomogeneity in the microstructure due to the dissimilar compositions and hence properties of the liquids. The larger MgO particles are converted to liquid at higher temperatures via the eutectic with molar ratio ~74:36 MgO:SiO_2 at 1850°C and the melting at 1890°C of any forsterite formed around the particles.

Table 7. Hot-pressing with 9 wt% of MgO, Al_2O_3 and Y_2O_3 in the molar composition 67:16:17 at 1750°C (theoretical density = 3·29 g cm^{-3})

Time (min)	*Weight loss (%)*	*Density (g cm^{-3})*	*XRD results*
5	0·9	2·60	$6H_{10}\,15R_{0\cdot6}\,4H_w\,J_{0\cdot2}$
15	2·2	2·90	$6H_{10}\,15R_{0\cdot6}\,4H_w\,J_{0\cdot4}$
30	1·6	3·07	$6H_{10}\,15R_{0\cdot6}\,4H_{0\cdot1}\,J_{0\cdot8}$
45	2·2	3·07	$6H_{10}\,15R_{0\cdot6}\,4H_w\,J_{0\cdot7}$
90	2·3	3·13	$6H_{10}\,15R_{0\cdot8}\,4H_{0\cdot1}\,J_{0\cdot5}$

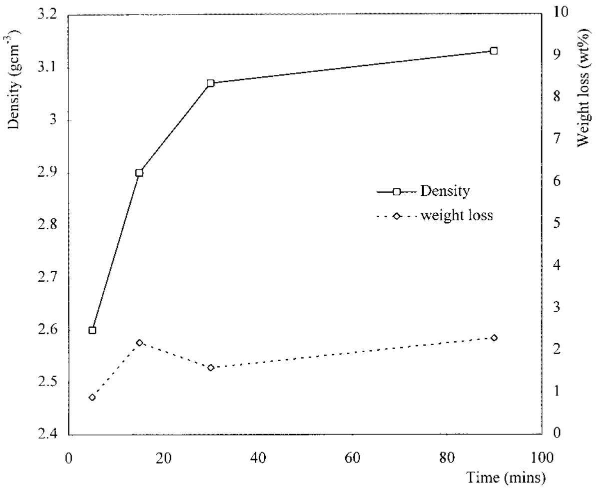

Fig. 7. Hot-pressing at 1750°C with 9 wt% of MgO, Al_2O_3 and Y_2O_3 (molar ratio 66:16:17).

Table 8. Hot-pressing with MgO, Al_2O_3 and Y_2O_3 (for 30 min with additives of molar composition 67:16:17)[a]

Additive size (wt%)	*Packing powder*	*Temp (°C)*	*Weight loss (wt%)*	*Density (g cm^{-3})*	*Theoretical density (g cm^{-3})*	*XRD results (additive phases only)*
3	BN	1750	1·0	2·58	3·24	—
6	BN	1750	1·6	2·93	3·26	$J_{0\cdot3}$
6	BN	1800	2·6	3·04	3·26	—
9	BN	1750	1·6	3·07	3·29	$J_{0\cdot8}$
9	BN	1800	2·3	3·21	3·29	J_1
3	BN, MgO, Al_2O_3 and Y_2O_3	1800	+1·5	3·18	3·24	$J_{0\cdot6}$
6	BN, MgO, Al_2O_3 and Y_2O_3	1800	+2·4	3·23	3·26	$J_{0\cdot7}$
9	BN, MgO, Al_2O_3 and Y_2O_3	1800	+1·4	3·23	3·29	$J_{0\cdot7}$

[a] The phase J resembles the YAM-type 'J-phase' (Table 4).

Table 9. Pressureless sintering with MgO, Al_2O_3 and Y_2O_3 (with 9 wt% of additive)

Additive composition (mol%)			*Temperature (°C)*	*Time (min)*	*Powder bed*	*Weight loss (wt%)*	*Density (g cm^{-3})*	*Theoretical density (g cm^{-3})*
MgO	*Al_2O_3*	*Y_2O_3*						
56	17	27	1750	180	BN,MgO,Al_2O_3,Y_2O_3	3·9	2·41	3·30
64	25	11	1750	180	BN	4·1	2·57	3·28
76	10	13	1750	180	BN	0·5	2·56	3·28
76	10	13	1800	140	BN,MgO,Al_2O_3,Y_2O_3	8·4	2·55	3·28
64	25	11	1850	120	BN	5·8	2·65	3·28
76	10	13	1850	120	BN	5·0	2·61	3·28
64	25	11	2000	60	BN	6·9	2·83	3·28
—	53	47	2000	30	BN,Al_2O_3,Y_2O_3	8·5	2·85	3·31

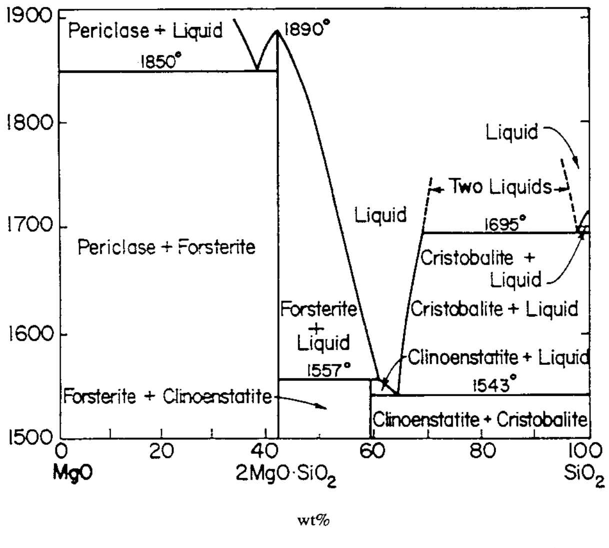

Fig. 8. Phase diagram for the system MgO–SiO_2.[8]

The increased liquid volume and the higher temperature result in a more efficient solution-reprecipitation stage, accounting for the higher density obtained at 1900°C.

Further evidence for the solution-reprecipitation process is seen in the stabilisation of the 4H SiC polytype at 1900°C (Table 1). The reprecipitated SiC is probably doped with Mg atoms from the liquid phase, and since Mg is an electron acceptor relative to SiC it is expected to stabilise the 4H polytype in a similar way to Al[9] and B.[10] The incorporation of Mg atoms in the 4H SiC is further evidenced by the slight distortion of the lattice, giving the cell parameter $c \approx 10{\cdot}09$ Å, similar to that obtained for 4H SiC containing ~0·4 wt% Al,[11] compared with the value of 10·061 Å for pure 4H SiC (ICDD card 29-1127). The cell dimension *a* was not measured due to the presence of overlapping 6H reflections. The lack of distortion of the 6H polytype suggests the incorporation of Mg in the newly deposited SiC rather than by diffusion into the existing grains.

The high weight losses undergone by the samples above 1750°C indicate volatilisation caused by reactions between the liquid phase and the SiC or the reducing atmosphere of the hot-press. The oxidation reaction for SiC having the lowest free energy between 1550 and 1950°C is reported by Negita[1] as:

$$SiC + 3/2O_2 \rightarrow SiO_2 + CO \qquad (1)$$

However, under these conditions, MgO has a tendency to dissociate into the elements, as given by:

$$3MgO \rightarrow 3Mg + 3/2O_2 \qquad (2)$$

The overall reaction will therefore be:

$$3MgO + SiC \rightarrow 3Mg + SiO_2 + CO \qquad (3)$$

indicating a general tendency for the MgO to react with the SiC and form SiO_2. The ΔG data given by Negita was calculated at 2400 K rather than the temperatures of 2000–2300 K used in this work, but the slopes of ΔG *vs.* T curves in this range are approximately similar, and therefore similar results can be expected at the lower temperatures. The additive liquid is therefore transient, limiting the time during which liquid phase densification may occur. The introduction of MgO in the packing powder may to some extent deter weight loss by generating high partial pressures of the gaseous products formed by the reduction of the MgO additive or by directly infiltrating the sample.

The introduction of Al_2O_3 as an additive also stabilises the MgO, reducing the fraction of MgO lost during hot-pressing. This could be achieved by a greater stability of the liquid phase or by the initial formation of spinel. In the latter case, greater weight losses would be expected for additives with high MgO contents, as these form little spinel. Since this is not the case, the results suggest a greater stability of the Al-containing liquid. The liquid phase is obtained via a eutectic in the $MgO–Al_2O_3–SiO_2$ system at 1710°C with the molar composition of 64:10:24 $MgO:Al_2O_3:SiO_2$,[12] agreeing well with the optimum additive composition of 88 mol% MgO assuming a silica content of ~3 wt% in the SiC powder, and to a lesser extent via other low-temperature eutectics at SiO_2-rich compositions.

A similar mechanism is assumed to enable densification with additions of MgO and Y_2O_3. The only reported eutectic between MgO and Y_2O_3 is at 2110°C[13] (with a composition of 50 mol% MgO). The high densities obtained with additives containing high ratios of MgO to Y_2O_3 suggest a eutectic in the system $MgO–Y_2O_3–SiO_2$ having a similar composition to that in the system $MgO–Al_2O_3–SiO_2$ and at a temperature below 1700°C. This is in agreement with the presence of a eutectic with the approximate molar composition of 5:1:3 $MgO:Y_2O_3:SiO_2$ in the tentative phase diagram given by Kuang *et al.*[14] on the basis of thermodynamical calculation.

Combined additions of MgO, Al_2O_3 and Y_2O_3 gave a further improvement in sample density. Phase diagrams for the systems $MgO–Al_2O_3–Y_2O_3$ and $MgO–Al_2O_3–Y_2O_3–SiO_2$ have not been reported, but the possibility of eutectics in the system $MgO–Al_2O_3–Y_2O_3$ offers the potential for low-temperature liquid formation independent of the SiO_2 content of the SiC powder. The rapid rise in shrinkage rate observed at ~1690°C suggests the formation of an extensive eutectic liquid. In order to determine whether this required the SiO_2 or not, an investigation of the system $MgO–Al_2O_3–Y_2O_3$ was carried out by sintering compacts of the oxide mixtures in a glass-making rig which allowed rapid cooling. The samples were packed in BN containing some MgO, Al_2O_3 and Y_2O_3, with a layer of pure BN immediately around the samples, allowing the weight losses to be kept below 6 wt%. A substantial liquid phase was seen at 1700–1730°C, confirming the presence of a eutectic or eutectics within the approximate composition range 40–70 mol% MgO, 10–30 mol% Al_2O_3 and 15–35 mol% Y_2O_3 (Fig. 9). This lies between reported eutectics in the systems $MgO–Al_2O_3$ and $MgO–Y_2O_3$, and overlaps the observed optimum additive composition range but is slightly lower in MgO, reflecting the loss of MgO during hot-pressing. No new ternary compounds were observed in the system $MgO–Al_2O_3–Y_2O_3$, and the phase J was not seen, reinforcing its identification as a YAM-type silicon oxynitride.

For all additive combinations, the results follow a typical Kingery liquid phase sintering process, with an initial period of rapid densification, due to the formation of a substantial amount of liquid phase, which promotes particle-rearrangement. This is followed, after around 30 min, by a transition to the slower process of solution-reprecipitation. Eventually, the densification slows almost to a standstill, because further sintering can only take place by solid state diffusional processes, which are very slow for SiC at temperatures below 2000°C. The transition to this final stage can be accelerated by the loss of the liquid phase due to volatilisation. The MgO is the most volatile of the additives, the loss of which drives the grain boundary phase composition away from the liquid-forming region and, for additions of MgO plus Y_2O_3 or MgO plus Y_2O_3 and Al_2O_3 towards that of the phase J.

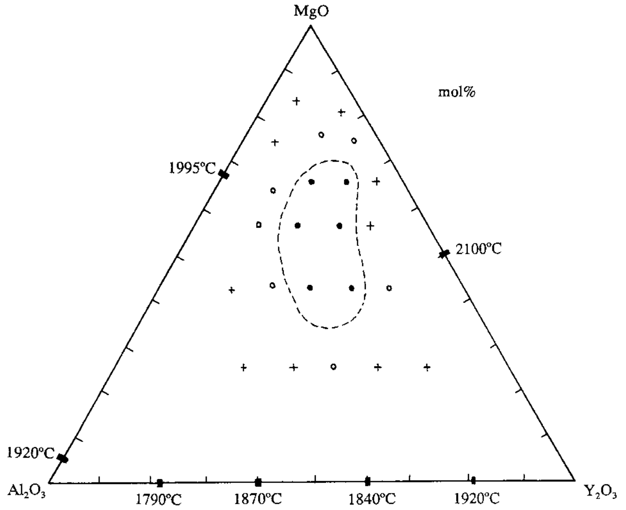

Fig. 9. Liquid forming region in the system $MgO–Al_2O_3–Y_2O_3$ at 1750°C.

In pressureless sintering the effect of the volatilisation of the MgO is too great and the escape of volatile products opposes densification, which can continue only through the liquid phase generated between Al_2O_3, Y_2O_3 and SiO_2 or by solid state diffusion. The use of powder beds containing the additive compounds had no beneficial effect. Weight losses are lower at 1750°C, with the retention of some MgO, but the limited rate of material transport through the liquid phase at this temperature and the absence of external pressure, as supplied by a hot-press, to augment the capillary pressure driving the particle rearrangement ensure that the densification is limited.

5 Conclusions

MgO promotes low temperature densification in hot-pressed α-SiC by particle rearrangement and subsequent solution-reprecipitation through a liquid phase formed between the additive and SiO_2 from the SiC grain surfaces. The efficiency of the liquid phase in promoting particle rearrangement suggests a good wettability and low viscosity, but the limited solubility of the SiC restricts the rate of solution and reprecipitation. A glassy phase is formed from the liquid on cooling.

The volatility of the additive through reaction with the SiC or the hot-press environment means that the liquid phase is transient above 1750°C, although this can be opposed by the introduction of MgO into the powder bed used to pack the sample.

Improved densification is obtained by the introduction of either Y_2O_3 or Al_2O_3 to the additive. Liquid phases were generated by eutectics at similar molar compositions in the systems MgO–$A1_2O_3$–SiO_2 and MgO–Al_2O_3–SiO_2 at temperatures of ~1700°C. The MgO was stabilised, reducing the weight losses and enabling prolonged solution and reprecipitation of the SiC in the liquid phase.

Additives comprising a mixture of MgO, Al_2O_3 and Y_2O_3 gave a further improvement in density. The optimum additive composition range was 60–80 mol% MgO, 10–25 mol%) Al_2O_3 and 10–25 Mol% Y_2O_3. This corresponds to a eutectic or eutectics at around 1700°C in the system MgO $A1_2O_3$–Y_2O_3, providing an extensive, relatively stable liquid phase independent of the SiO_2 content of the SiC powder. Pressureless sintering with such an additive combination was unsuccessful, however, due to the volatilisation of the additives.

Acknowledgements

We thank EA Technology for collaborating as the CASE sponsor in the project of which the present study formed a part. More specifically, we thank Mrs Ruth Wroe of EA for numerous useful discussions and for advice and practical assistance during the course of the work.

References

1. Negita, K., Effective sintering aids for silicon carbide ceramics: reactivities of silicon carbide with various additives. *J Am. Ceram. Soc.*, 1986, **69**(12), C308–310.
2. Trigg, M. B., Dietrich, R., Drennan, J., Hay, D. G. and Oh, C.H., Dense SiC ceramic products, International Patent No: WO 91/06515, 16th May 1991.
3. Wild, S., Grieveson, P., Jack, K. H. and Latimer, M. J., The role of magnesia in the hot-pressing of silicon nitride. In *Special Ceramics 5*, ed. P. Popper. Brit. Ceram. Res. Assoc., 1972, pp. 377–389.
4. Kossowsky, R., Creep and fatigue of Si_3N_4 as related to microstructures. In *Ceramics for High Performance Applications, Proc. 2nd. Army. Mater. Tech. Conf.*, ed. J. J. Burke, A. E. Gorum and N. R. Katz. Brook Hill, 1974, pp. 347–371.
5. Lange, F. F., Silicon nitride polyphase systems: fabrication, microstructure and properties. *Int. Met. Rev.*, 1980, **25**(1), 1–20.
6. Kingery, W. D., Densification during sintering in the presence of a liquid phase. 1: theory. *J Appl. Phys.*, 1959, **30**(3), 301–306.
7. Sigl, L. S. and Kleebe, H.-J., Core/rim structure of liquid-phase-sintered silicon carbide. *J. Am. Ceram. Soc.*, 1993, **46**(3), 773–776.
8. Greig, J. W., In *Phase Diagrams for Ceramists*, ed. E. M. Levin, C. R. Robbins, H. F. McMurdie and M. K. Reser. Am. Ceram. Soc., 1964, Fig. 266.
9. Lundquist, D., On the structure of silicon carbide and its content of impurities. *Acta. Chem. Scan.*, 1948, **2**, 177–191.
10. Martin, S., Aspects of the hot-pressing of silicon carbide. Ph.D. thesis. University of Cambridge, 1980.
11. Mitomo, M., Inomata, Y. and Tanaka, H., Effect of aluminium on the stability of 4H- and 6H-silicon carbide at 2200°C. *Yogyo-Kyokai-Shi.*, 1970, **78**, 365–369.
12. Osborn, E. F. and Muan, A., In *Phase Diagrams for Ceramists*, ed. E. M. Levin, C. R. Robbins, H. F. McMurdie and M. K. Reser. Am. Ceram. Soc., 1964, Fig. 1712.
13. Tresvyatskii, S. G., Lopato, L. M., Ogorodnikova, A. A. and Shevchenko, A. V., In *Phase Diagrams for Ceramists Volume IV*, ed. R. S. Roth, T. Negas and L. P. Cook. Am. Ceram. Soc., 1981, Fig. 5156.
14. Kuang, S., Lukas, H. L., Hoffman M. J. and Petzow, G., Thermodynamical calculation of the MgO–Y_2O_3–SiO_2 system. In *Ceramic Materials and Components for Engines, Proc. 5th. Int. Symp.*, ed. D. S. Yan, X. R. Fu and S. X. Shi. World Scientific, 1995, pp. 446–449.